


# Co-expression of LKB1, MO25 $\alpha$ and STRAD $\alpha$ in bacteria yield the functional and active heterotrimeric complex

## Journal Article

**Author(s):**

Neumann, Dietbert; Suter, Marianne; Tuerk, Roland; Riek, Uwe; [Wallimann, Theo](#) 

**Publication date:**

2007-07

**Permanent link:**

<https://doi.org/10.3929/ethz-b-000413265>

**Rights / license:**

[In Copyright - Non-Commercial Use Permitted](#)

**Originally published in:**

Applied Biochemistry and Biotechnology. Part B, Molecular Biotechnology 36(3), <https://doi.org/10.1007/s12033-007-0029-x>

## Co-expression of LKB1, MO25 $\alpha$ and STRAD $\alpha$ in bacteria yield the functional and active heterotrimeric complex

Dietbert Neumann · Marianne Suter ·  
Roland Tuerk · Uwe Riek · Theo Wallimann

Published online: 25 May 2007  
© Humana Press Inc. 2007

**Abstract** The tumour suppressor LKB1 plays a critical role in cell proliferation, polarity and energy metabolism. LKB1 is a Ser/Thr protein kinase that is associated with STRAD and MO25 *in vivo*. Here, we describe the individual expression of the three components of the LKB1 complex using monocistronic vectors and their co-expression using tricistronic vectors that were constructed from monocistronic vectors using a fully modular cloning approach. The data show that among the three individually expressed components of the LKB1 complex, only MO25 $\alpha$  can be expressed in soluble form, whereas the other two, LKB1 and STRAD $\alpha$  are found almost exclusively in inclusion bodies. However, using the tricistronic vector system, functional LKB1-MO25 $\alpha$ -STRAD $\alpha$  complex was expressed and purified from soluble extracts by sequential immobilized-metal affinity and heparin chromatography, as shown by Western blotting using specific antibodies. In size exclusion chromatography, MO25 $\alpha$  and STRAD $\alpha$  exactly co-elute with LKB1 with an apparent molecular weight of the heterotrimeric complex of 160 kDa. The specific activity in the peak fraction of the size exclusion chromatography was 250 U/mg at approximately 25% purity. As shown by autoradiography, LKB1 and STRAD $\alpha$ , both strongly autophosphorylate *in vitro*. Moreover, recombinant LKB1 complex activates AMPK by phosphorylation of the  $\alpha$ -subunit at the Thr-172 site as shown (i) by Western blotting using phospho-specific antibodies after LKB1-dependent phosphorylation, (ii) by LKB1-dependent incorporation of radioactive phosphate into the  $\alpha$ -subunit of kinase dead AMPK heterotrimer, and (iii) by

activity determination of AMPK. Functional mammalian LKB1 complex is constitutively active, and when enriched from bacteria should prove to be a valuable tool for studying its molecular function and regulation.

**Keywords** Polycistronic · Heterotrimer · Protein complex · LKB1 · Tumour suppressor kinase

### Abbreviations

AMPK	AMP-activated protein kinase
IMAC	immobilized metal-ion affinity chromatography
SAMS	the synthetic peptide substrate of AMPK corresponding to the sequence HMRSAMSGHLVLRKRR
SDS-PAGE	sodium dodecylsulfate polyacrylamide gel electrophoresis
LKB1	the tumour suppressor kinase, also called STK11
LKBtide	synthetic peptide LSNLYHQGKFLQTFGSPYLRKRR
CaMKK	Ca <sup>2+</sup> /calmodulin-dependent protein kinase kinase
GST	glutathione-S-transferase
SAMS	synthetic peptide HMRSAMSGHLVLRKRR
MO25	mouse protein 25
SEC	size exclusion chromatography
STRAD	STE-20 related adaptor protein

### Introduction

Mutations in the *LKB1* (also called *STK11*) tumour suppressor gene, which encodes a Ser/Thr protein kinase, cause the Peutz-Jeghers cancer syndrome (PJS) [1, 2].

D. Neumann (✉) · M. Suter · R. Tuerk · U. Riek · T. Wallimann  
ETH Zurich, Institute of Cell Biology, HPM D23, Schafmattstr.  
18, Zurich 8093, Switzerland  
e-mail: dietbert.neumann@cell.biol.ethz.ch

Recent work identified LKB1 as a multitasking protein kinase playing important roles in cell proliferation, polarity and energy metabolism (reviewed in [3]). The cellular localization and activity of LKB1 is likely controlled through its interaction with a pseudokinase, termed STRAD, and an armadillo repeat-containing protein, named mouse protein 25 (MO25) [3]. Both, MO25 and STRAD, occur in two different isoforms,  $\alpha$  and  $\beta$  [4]. Genetic and biochemical findings indicate that LKB1 phosphorylates and thereby activates 14 protein kinases, all related to the AMP-activated protein kinase (AMPK) [5, 6].

Much recent research has focused on the cellular role of LKB1, but information about the kinase molecule itself is still lacking, partly due to the limited availability of the purified LKB1 protein complex. Bacterial expression of fusion proteins corresponding to LKB1 with hexahistidine, GST and MBP tags resulted either in insoluble aggregates or heavily degraded protein that were found to be non-functional [7]. We recently developed a polycistronic expression strategy for co-expression of multiple proteins in *E. coli* and, using this system, successfully produced functional heterotrimeric AMPK [8, 9], a fuel sensor of the cell and master regulator of energy metabolism [10]. AMPK is also a direct physiological target of LKB1 [11–14]. Moreover, the LKB1 tumour suppressor function might relate to inhibition of cell proliferation in response to low-cellular energy levels by deregulation of AMPK that is acting upstream of mTOR, the mammalian target of rapamycin [15–17]. Here, we set out on establishing a bacterial co-expression system for the functional LKB1 complex consisting of LKB1, MO25 $\alpha$  and STRAD $\alpha$ .

## Materials and methods

### Construction of expression vectors

Modified pET-vectors were used as described previously [9]. Briefly, the cDNAs encoding LKB1, MO25 $\alpha$  and STRAD $\alpha$  (GenBank Accession No. NM\_011492, BC020570, AF308302) were subcloned by PCR and inserted into the NdeI/SpeI sites of pET3ax (resulting in pLKB1, pMO25 $\alpha$  and pSTRAD $\alpha$ ) or in the NdeI/SpeI sites of pET14bx (resulting in pHis-LKB1, pHis-MO25 $\alpha$  and pHis-STRAD $\alpha$ ). The following primers were utilized for subcloning: 5'LKB1, AAA AAA CAT ATG GAC GTG GCG GAC CCC G; 3'LKB1, AAA AAA CTA GTT ACT GCT GCT TGC AGG CCG AG; 5'MO25 $\alpha$ , AAA AAC ATA TGC CGT TCC CGT TTG GGA AGT; 3'MO25 $\alpha$ , AAA AAC TAG TTA AGC TTC TTG CTG AGC TGG TCT CTT; 5'STRAD $\alpha$  AAA AAC ATA TGT CAT TTC TTG TAA GTA AAC CAG AGC GAA TCA GG; 3'STRAD $\alpha$ , AAA AAC TAG TTA GAA CTC CCA ATC GTC CAC CTC C (recognition sequences of NdeI

and SpeI underlined). Open reading frames of all constructs were sequenced utilizing the BigDye<sup>TM</sup> Terminator Cycle Sequencing Kit (PE Applied Biosystems, Rotkreuz, Switzerland) in an ABI Prism 310 Sequencer according to the manufacturers instructions. The monocistronic vectors were used for construction of the tricistronic expression vectors by repetitive subcloning cycles as described in Fig. 1. Plasmid constructs are listed in Table 1.

### Expression and purification of LKB1, MO25 $\alpha$ and STRAD $\alpha$

Plasmids pHis-LKB1, pHis-MO25 $\alpha$  and pHis-STRAD $\alpha$  encoding N-terminally hexahistidine-tagged LKB1, MO25 $\alpha$  and STRAD $\alpha$ , respectively, were transformed into competent host cells (*E. coli* BL21-Star<sup>TM</sup>(DE3), Invitrogen, Basel, Switzerland) and incubated overnight at 37°C on LB agar containing 150  $\mu$ g/ml ampicillin. Resuspended

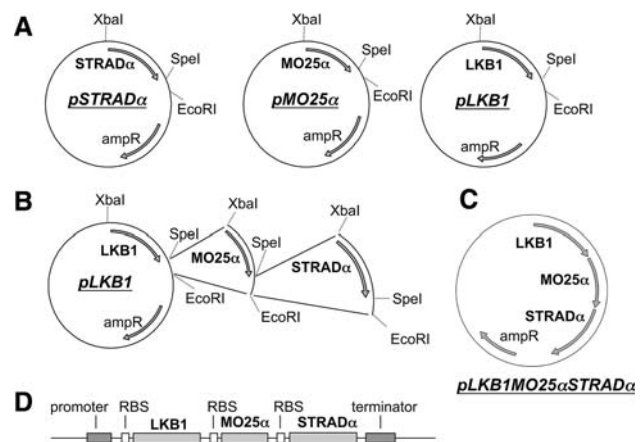


**Fig. 1** Cloning scheme for construction of the tricistronic expression vector. **(A)** The cDNA sequences encoding LKB1, MO25 $\alpha$  and STRAD $\alpha$  were subcloned into individual pET-plasmids, harboring an ampicillin resistance gene (amp<sup>r</sup>) and carrying a SpeI-site, which results in the monocistronic vectors termed ‘pLKB1’, ‘pMO25 $\alpha$ ’ and ‘pSTRAD $\alpha$ ’. These vectors are suitable for bacterial expression of individual proteins. Each of the monocistronic vectors may also encode an N-terminal hexahistidine-tag (termed ‘pHis-LKB1’, ‘pHis-MO25 $\alpha$ ’ and ‘pHis-STRAD $\alpha$ ’) to facilitate protein purification. **(B)** Any of the monocistronic vectors can be used to accept XbaI/EcoRI fragments harboring a functional cistron and encoding any of the other proteins by restriction with SpeI/EcoRI and ligation. As XbaI and SpeI sites are compatible but not reCleavable by either of the restriction enzymes, the introduction of a third cistron can follow the same scheme. Successive restriction and ligation of individual cistrons, encoding MO25 $\alpha$  and STRAD $\alpha$ , using the acceptor vector pLKB1 leads to the final tricistronic vector **(C)** pLKB1MO25 $\alpha$ STRAD $\alpha$ . **(D)** The tricistronic gene construct consists of a promoter, ribosome binding sites (RBS), the open reading frames of LKB1, MO25 $\alpha$  and STRAD $\alpha$ , as well as a transcriptional terminator. The three restriction sites necessary for cloning are indicated and plasmid names are underlined. Plasmid maps are not drawn to scale. The cloning scheme is a variation of the method in Ref. [9] using *EcoRI* instead of *BlnI* for uniqueness of the former site in all open reading frames and vector sequence

**Table 1** Overview of plasmids used throughout this study

Plasmid	Insert/Modification
pET3ax	Introduction of SpeI site to pET3a
pET14bx	Introduction of SpeI site to pET14b
pLKB1	LKB1 subcloned into the NdeI/SpeI sites of pET3ax
pMO25 $\alpha$	MO25 $\alpha$ subcloned into the NdeI/SpeI sites of pET3ax
PSTRAD $\alpha$	STRAD $\alpha$ subcloned into the NdeI/SpeI sites of pET3ax
pHis-LKB1	LKB1 subcloned into the NdeI/SpeI sites of pET14bx
pHis-MO25 $\alpha$	MO25 $\alpha$ subcloned into the NdeI/SpeI sites of pET14bx
pHis-STRAD $\alpha$	STRAD $\alpha$ subcloned into the NdeI/SpeI sites of pET14bx
pLKB1MO25 $\alpha$	pLKB1 digested with SpeI/EcoRI and ligated to XbaI/EcoRI-fragment of pMO25 $\alpha$
pHis-LKB1MO25 $\alpha$	pHis-LKB1 digested with SpeI/EcoRI and ligated to XbaI/EcoRI-fragment of pMO25 $\alpha$
pLKB1His-MO25 $\alpha$	pLKB1 digested with SpeI/EcoRI and ligated to XbaI/EcoRI-fragment of pHis-MO25 $\alpha$
pLKB1MO25 $\alpha$ STRAD $\alpha$	pLKB1MO25 $\alpha$ digested with SpeI/EcoRI and ligated to XbaI/EcoRI-fragment of pSTRAD $\alpha$
pHis-LKB1MO25 $\alpha$ STRAD $\alpha$	pHis-LKB1MO25 $\alpha$ digested with SpeI/EcoRI and ligated to XbaI/EcoRI-fragment of pSTRAD $\alpha$
pLKB1His-MO25 $\alpha$ STRAD $\alpha$	pLKB1His-MO25 $\alpha$ digested with SpeI/EcoRI and ligated to XbaI/EcoRI-fragment of pSTRAD $\alpha$
pLKB1MO25 $\alpha$ His-STRAD $\alpha$	pLKB1MO25 $\alpha$ digested with SpeI/EcoRI and ligated to XbaI/EcoRI-fragment of pHis-STRAD $\alpha$

cells of each plate were used to inoculate 1 l auto-induction medium ZYM-5052 as described by Studier [18]. Cultures were grown in a shaker incubator at 37°C and 350 rpm. Cells were harvested after growth overnight, resuspended in lysis buffer (50 mM Na-phosphate pH 8.0, 150 mM NaCl, 10 mM imidazole, 1 mM  $\beta$ -mercaptoethanol) and sonicated on ice in a Branson 250 sonifier (50% duty, output 5, 2 min, 3 times). For purification of hexahistidine-tagged MO25 $\alpha$  insoluble material was removed by centrifugation and the supernatant was loaded onto Ni-NTA agarose (Qiagen, Basel, Switzerland). The column was washed (three column volumes with lysis buffer, containing 20 mM imidazole) and eluted (lysis buffer, containing 250 mM imidazole). For purification of hexahistidine-tagged LKB1 and STRAD $\alpha$ , the insoluble material was collected by centrifugation after lysis and resuspended in lysis buffer containing 0.1% Triton X-100. After repetitive sonication, centrifugation and resuspension (3 times), the pellet was collected by centrifugation and solubilized in denaturing buffer containing 6 M guanidine hydrochloride (Gu-HCl), 20 mM imidazole and 50 mM Na-phosphate, pH 8.0. After centrifugation, the supernatant was loaded on a 5 ml Ni<sup>2+</sup>-charged HiTrap Chelating HP column (GE Healthcare Europe, Otelfingen, Switzerland), washed with 20 ml denaturing buffer and eluted with denaturing buffer containing 250 mM imidazole. Pooled elution fractions of each protein were stored at -20°C until usage. Prior to analysis by SDS-PAGE, 6 M Gu-HCl was removed by dialysis against 8 M Urea.

Co-expression of LKB1, MO25 $\alpha$  and STRAD $\alpha$ : small scale expressions

The tricistronic plasmids pLKB1MO25 $\alpha$ STRAD $\alpha$ , pHis-LKB1MO25 $\alpha$ STRAD $\alpha$ , pLKB1His-MO25 $\alpha$ STRAD $\alpha$  and

pLKB1MO25 $\alpha$ His-STRAD $\alpha$  were transformed into competent host cells (*E. coli* BL21-Star<sup>TM</sup>(DE3), Invitrogen, Basel, Switzerland) and incubated overnight at 37°C on LB agar. For co-expression of bacterial chaperones competent Tuner(DE3) cells, or Tuner(DE3) cells harboring either pOFXT7-SL2 or pOFXT7-KJE2 [19], were transformed with pHis-LKB1MO25 $\alpha$ STRAD $\alpha$ . Appropriate antibiotics were added at the following concentrations: 150  $\mu$ g/ml ampicillin and 25  $\mu$ g/ml chloramphenicol. Resuspended cells of each plate were used to inoculate 1 l auto-induction medium ZYM-5052 as described by Studier [18], cells were collected and lysed by sonication. Soluble fractions were analyzed by SDS-PAGE and Coomassie Blue-staining or Western-blotting followed by immuno-detection as described below.

Co-expression of LKB1, MO25 $\alpha$  and STRAD $\alpha$  and purification of the complex

The tricistronic plasmid pHis-LKB1MO25 $\alpha$ STRAD $\alpha$  was transformed into competent host cells (*E. coli* BL21-Star<sup>TM</sup>(DE3), Invitrogen, Basel, Switzerland) and incubated overnight at 37°C on LB agar containing 150  $\mu$ g/ml ampicillin. Resuspended cells were used for inoculation of 800 ml M9\* medium (25.5 g/l Na<sub>2</sub>HPO<sub>4</sub>\*2H<sub>2</sub>O, 9 g/l KH<sub>2</sub>PO<sub>4</sub>, 1 g/l NH<sub>4</sub>Cl, 0.5 g/l NaCl, 2 mM MgSO<sub>4</sub>, 0.5% w/v glucose, 2 ml/l TE and 150 mg/l ampicillin) and agitated in shaker flasks at 37°C at 250 rpm. After 24 h growth the cells were used for inoculation of a 42 l bioreactor (MBR Switzerland 1982) containing 27 l Riesenberg medium (13.3 g/l KH<sub>2</sub>PO<sub>4</sub>, 4.0 g/l (NH<sub>4</sub>)<sub>2</sub>HPO<sub>4</sub>, 1.7 g/l citric acid, 1.5 ml polypropylene glycol 2000 as antifoam, supplemented with 2 ml/l 2M MgSO<sub>4</sub>, and

150 mg/l ampicillin) with 1.7% (w/v) glucose. Titration with 35% NH<sub>4</sub>OH and 30% H<sub>3</sub>PO<sub>4</sub> was used to keep pH constant at 7.2. Trace element solution (TE) containing 1 M HCl, 7.6 mM MnCl<sub>2</sub>, 3.6 mM ZnSO<sub>4</sub>, 4.8 mM H<sub>3</sub>BO<sub>3</sub>, 1.2 mM Na<sub>2</sub>MoO<sub>4</sub>, 0.9 mM CoCl<sub>2</sub>, 2.26 mM Na<sub>2</sub>EDTA, 37.1 mM CaCl<sub>2</sub>, 15.9 mM FeSO<sub>4</sub>, 10 mM CoSO<sub>4</sub>, 2 mM H<sub>2</sub>SeO<sub>3</sub>, was added to final amount of 2 ml/l culture. Cells were batch grown for 12 h at 34°C until depletion of glucose and acetate (pO<sub>2</sub> ~ 100%). After start of 65% (w/v) glucose feed, TE solution and 2 ml/l 2 M MgSO<sub>4</sub> were added. The feed was balanced with O<sub>2</sub> consumption until onset of pO<sub>2</sub> limitation at a mass flow air of 45 l/min with overpressure of 0.5 bar and at stirrer maximum of 1000 rpm. Further TE solution and 1 ml/l 2 M MgSO<sub>4</sub> were added each 15–20 OD<sub>600nm</sub>'s and after induction each 2.5 h. Growth temperature was reduced to 27°C and cells were induced with 50 mg/l IPTG at OD<sub>600nm</sub> = 36 for 7 h. Cells were harvested by centrifugation, washed in 0.9% (w/v) NaCl solution and centrifuged again. The final cell pellet was frozen in liquid nitrogen and stored at –20°C until usage. A bacterial cell pellet corresponding to 100 g wet weight was resuspended in ice-cold lysis buffer (15% sucrose w/v, 50 mM Naphosphate pH 8.0, 30% (w/v) glycerol, 10 mM imidazole, 1 mM β-mercaptoethanol). Cells were lysed in a high-pressure homogenizer (EmulsiFlex-C5, Avestin, Canada) at 1000 bar. Insoluble material was removed by centrifugation and the supernatant was loaded onto Ni-NTA agarose (Qiagen, Basel, Switzerland). The column was washed with three column volumes of lysis buffer, containing 20 mM imidazole and eluted with lysis buffer, containing 250 mM imidazole. Pooled Ni-NTA elution fractions were diluted 20-fold with heparin loading buffer (100 mM NaCl, 10 mM Tris-Cl, pH 7.2) and loaded onto a 1 ml HiTrap Heparin column (GE Healthcare Europe, Otelfingen, Switzerland). Protein was eluted with heparin elution buffer (1M NaCl, Tris-Cl, pH 7.2) and elution fractions were stored at 4°C until further analysis. Snap freezing in liquid nitrogen is possible without significant loss of kinase activity, but repeated freeze and thaw cycles are not recommended.

#### Size exclusion chromatography

A heparin elution fraction containing LKB1 complex was subjected to size exclusion chromatography (SEC). About 1.2 mg of partly purified LKB1 complex were separated in 250 mM NaCl, 2 mM MgCl<sub>2</sub>, 1 mM dithiothreitol and 10 mM Tris-Cl, pH 7.2 at a flow rate of 0.5 ml min<sup>-1</sup> and a temperature of 7°C with a Superose 12 HR 10/30 column connected directly between the UV/VIS flow cell and the injection valve of an Äkta Explorer 100 Air HPLC system (GE Healthcare Europe, Otelfingen, Switzerland). The column was calibrated for molecular weight with the

following marker proteins (GE Healthcare Europe, Otelfingen, Switzerland): carbonic anhydrase (29 kDa), bovine serum albumin (67 kDa), alcohol dehydrogenase (150 kDa), β-amylase (200 kDa), apoferritin (443 kDa) and thyroglobulin (669 kDa).

#### SDS-PAGE and Western blotting

Protein samples were diluted in Laemmli SDS sample buffer and snap frozen in liquid nitrogen at indicated time points. After SDS-PAGE (12% polyacrylamide) and transfer to Protran® BA85 nitrocellulose membranes (Whatman, Bottmingen, Switzerland), the membranes were blocked in TBS (20 mM Tris-HCl, pH 7.5, 150 mM NaCl) with 5% low-fat milk powder or bovine serum albumin. The antibodies were applied in the same buffer at various dilutions and the blots were incubated for 2–16 h. After extensive washing in TBS, blots were incubated for 1 h at room temperature with horseradish peroxidase-coupled secondary antibodies. After repeated extensive washing, signals were detected with enhanced chemiluminescence (Applichem, Axon Lab, Baden-Dättwil, Switzerland) and Kodak X-ray-sensitive films (Kodak SA, Renens, Switzerland). The following primary and secondary antibodies were used at appropriate dilution: goat anti-LKB1 (Santa Cruz, Cat. No. sc-5637), sheep anti-MO25α and anti-STRADα were purchased from Dr. Alessi, Dundee, mouse Penta-His antibody (Qiagen, Cat No. 34660), rabbit anti-AMPKγ was a kind gift of Dr. David Carling, phospho-specific AMPKα Thr-172 monoclonal antibodies (Cell Signaling Technology, BioConcept, Allschwil, Switzerland), goat anti-mouse peroxidase conjugated (Pierce, Perbio Science, Lausanne, Switzerland), goat anti-rabbit peroxidase conjugated (Calbiochem, VWR, Dietikon, Switzerland), and mouse anti-goat/sheep peroxidase conjugated (Sigma/Fluka, Buchs, Switzerland).

#### Kinase activity determination

Protein fractions containing recombinant LKB1 complex were assayed using LKBtide (an artificial peptide substrate corresponding to the sequence LSNLYHQGKFLQTFCC SPLYRRR) and non-radioactive ATP. The buffer for LKB1 activity determination consisted of 100 mM HEPES, pH 7.1, 1 mM DTT, 5 mM MgCl<sub>2</sub>, 1 mM ATP, 250 μM LKBtide. LKB1 activity assays were performed in Eppendorf tubes on a thermal shaker at 30°C and 300 rpm. After incubation (10 or 20 min) the assay mixture was snap frozen in liquid nitrogen and stored at –20°C until further analysis. The amount of non-phosphorylated and phosphorylated LKBtide was quantified by HPLC analysis, analogous to AMPK activity determination as reported previously [20]. Briefly, a cation exchange column (Source



15S, 1 ml, from GE Healthcare Europe, Otelfingen, Switzerland) in a HPLC-system equipped with two independent UV/VIS spectrometers (Shimadzu, Reinach, Switzerland) was used for separation and quantitation of peptides. Samples were eluted with a linear gradient (0–0.5 M NaCl in 5 mM Na-phosphate, pH 3.0 containing 15% acetonitrile), and monitored at 280 and 220 nm. The latter wavelength was used for quantitation, because absorbance of peptide bonds at 220 nm is much stronger than that of aromatic amino acids at 280 nm. LKB1 activities were calculated from HPLC chromatograms by integration of the peak corresponding to phosphorylated LKBtide. AMPK-activity was assessed with SAMS-peptide as substrate as described recently [20].

### Expression and purification of AMPK

Wild-type AMPK  $\alpha 1\beta 1\gamma 1$ ,  $\alpha 2\beta 2\gamma 1$ , and kinase-defective mutant AMPK  $\alpha 1D157A\beta 1\gamma 1$  were bacterially expressed and purified on Ni-NTA superflow columns (Qiagen, Basel, Switzerland) following the procedure described in Ref. [9]. AMPK was further processed to highest purity and stock solutions of the enzyme were kept in 50% glycerol at  $-20^{\circ}\text{C}$ .

### Phosphorylation of AMPK by LKB1

Autophosphorylation of LKB1 complex (using the heparin elution peak fraction) was performed for 30 min at  $30^{\circ}\text{C}$  in assay buffer containing 200  $\mu\text{M}$  ATP, 50  $\mu\text{M}$  AMP, 5 mM  $\text{MgCl}_2$ , 1 mM DTT and 10 mM HEPES, pH 7.4. The reaction volume was doubled using assay buffer supplemented with  $\gamma^{32}\text{P}$ -ATP (specific activity of 1.35 mCi/ml) and 500 ng of AMPK. After incubation for 10 min at  $37^{\circ}\text{C}$ , the reactions were stopped by addition of Laemmli SDS sample buffer and immediate heating at  $95^{\circ}\text{C}$  for 5 min. Aliquots of 400 ng AMPK were subjected to SDS-PAGE and autoradiography. Briefly, Coomassie-stained gels were dried on 3MM Chr paper (Whatman, Böttmingen, Switzerland) and exposed to BioMax MR films (Kodak SA, Renens, Switzerland) at  $-80^{\circ}\text{C}$  for 14 h. The residual 100 ng of AMPK were separated by SDS-PAGE and Western-blotting was performed as described above.

## Results

### Expression of LKB1, MO25 $\alpha$ and STRAD $\alpha$ in *E. coli*

In this study, a bacterial co-expression strategy was attempted to yield functional LKB1-MO25 $\alpha$ -STRAD $\alpha$  protein complex. The cloning procedure for construction of a tricistronic gene starts by construction of monocistronic

expression vectors (Fig. 1). Individual plasmids encoding for either hexahistidine-tagged LKB1, MO25 $\alpha$  or STRAD $\alpha$  were used first to produce these proteins separately in *E. coli*. After expression, lysis and centrifugation, soluble and insoluble fractions of the respective individual proteins were analyzed by SDS-PAGE and Western-blotting using antibodies recognizing the hexahistidine-tag (Fig. 2). The results show that most of the MO25 $\alpha$  protein was found in the soluble fraction, whereas only a very small fraction of LKB1, and even partly degraded, was found in the soluble extract, and no soluble STRAD $\alpha$  was detectable at all (Fig. 2B, lanes 1–3). Thus, immobilized metal-ion affinity chromatography (IMAC) was used to purify MO25 $\alpha$  from soluble extracts, whereas LKB1 and STRAD $\alpha$  were solubilized from inclusion bodies prior to purification under denaturing conditions. Eluates were analyzed by SDS-PAGE and Western blotting (Fig. 3). The Coomassie Blue-stained gel reveals high purity of the individual proteins after single step purification (Fig. 3A). The theoretical molecular weights of MO25 $\alpha$  (39.9 kDa) and STRAD $\alpha$  (48.4 kDa) correspond well to the estimated apparent molecular weights of 40 and 50 kDa, respectively (Fig. 3, lanes 2 and 3). In accordance with an earlier report [7], the observed apparent molecular weight of LKB1 in SDS-PAGE is around 60 kDa (Fig. 3A, lane 1), which is higher than the expected 49.3 kDa even if taking into account the hexahistidine-tag (51.4 kDa). Specific antibodies raised either against LKB1, MO25 $\alpha$  or STRAD $\alpha$  clearly show immunoreactivity against their corresponding immunogens (Fig. 3B–D) at the molecular weight of the protein bands as seen in the Coomassie Blue-stained gel (Fig. 3A). Western-blot of hexahistidine-tagged LKB1 and STRAD $\alpha$  that were purified from inclusion bodies both show additional signals with higher electrophoretic mobility in SDS-PAGE indicating possible degradation products. As these peptides were immunoreactive with antibodies recognizing the N-terminal hexahistidine-tag (Fig. 3E), they are likely due to C-terminal truncations. Expectedly, the antibodies that recognize the hexahistidine-tag show a signal for LKB1, MO25 $\alpha$  and STRAD $\alpha$  at the same position on the Western-blot that was recognized by the protein-specific antibody (compare Fig. 3B–D with E). Taken together, hexahistidine-tagged LKB1, MO25 $\alpha$  and STRAD $\alpha$  have been bacterially expressed and purified by single step IMAC, and the corresponding antibodies specifically recognize their immunogens on Western-blot. Our data show that from the three individually expressed components of the LKB1 complex, only MO25 $\alpha$  can be obtained in soluble form in significant quantities, whereas the other two, LKB1 and STRAD $\alpha$ , are found preferentially in the insoluble fraction.

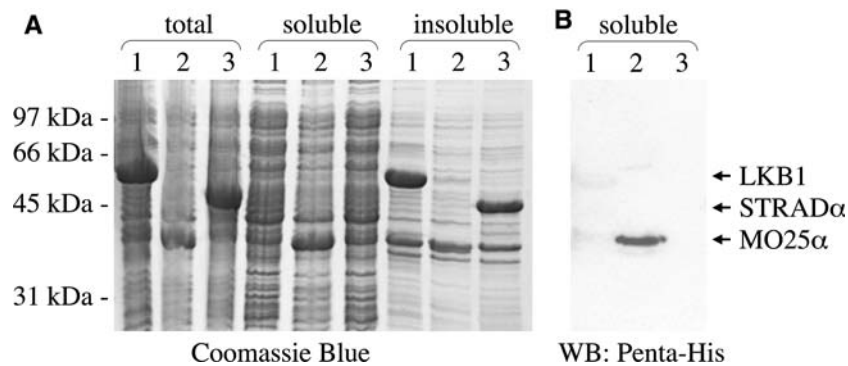


**Fig. 2** Solubility analysis of LKB1, MO25 $\alpha$  and STRAD $\alpha$  after expression from individual monocistronic vectors. Plasmids encoding hexahistidine-tagged LKB1 (lanes 1), MO25 $\alpha$  (lanes 2) or STRAD $\alpha$  (lanes 3), were transformed to competent *E. coli* and harvested after overnight expression in auto-inducing media. After lysis the total,

soluble and insoluble bacterial extracts were analyzed by SDS-PAGE. (A) Coomassie Blue stained gel. (B) Immuno-detection of proteins after Western-blotting using antibodies recognizing the hexahistidine-tag

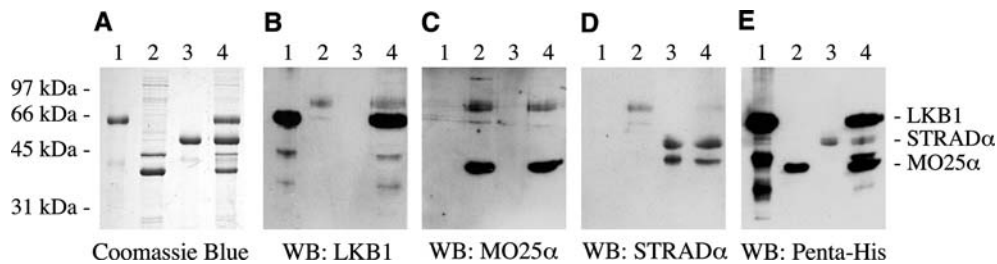


**Fig. 3** Purification of separate LKB1, MO25 $\alpha$  or STRAD $\alpha$  proteins and evaluation of antibodies. Hexahistidine-tagged LKB1, MO25 $\alpha$  and STRAD $\alpha$  were expressed individually in bacteria using the monocistronic vectors pHis-LKB1, pHis-MO25 $\alpha$  and pHis-STRAD $\alpha$ , respectively. LKB1 and STRAD $\alpha$  accumulated in inclusion bodies and were purified under denaturing conditions by IMAC, whereas

MO25 $\alpha$  was partly soluble and was purified from soluble extracts by IMAC (not shown). Purified proteins were analyzed by SDS-PAGE followed by Coomassie-Blue staining (A) or Western-blotting (B–E). Separate Western-blot were prepared for probing with four different antibodies as indicated. Lane 1, LKB1; lane 2, MO25 $\alpha$ ; lane 3, STRAD $\alpha$ ; lane 4: LKB1, MO25 $\alpha$  and STRAD $\alpha$  (1  $\mu$ g each)

#### Co-expression of LKB1, MO25 $\alpha$ and STRAD $\alpha$ : Positional effect of hexahistidine-tag

A series of tricistronic plasmids encoding for all three subunits of the LKB1 complex, with either none or a single subunit hexahistidine-tagged (pLKB1MO25 $\alpha$ STRAD $\alpha$ , pHis-LKB1MO25 $\alpha$ STRAD $\alpha$ , pLKB1His-MO25 $\alpha$ STRAD $\alpha$ , pLKB1MO25 $\alpha$ His-STRAD $\alpha$ ), were constructed following the cloning scheme shown in Fig. 1. After transformation of such tricistronic plasmids into bacteria and overnight growth in auto-inducing media [18], the expression levels of all subunits in soluble extracts were evaluated by Western-blotting after SDS-PAGE (Fig. 4). Despite co-expression of all three subunits of the LKB1 complex, LKB1 and STRAD $\alpha$  were not detectable in the supernatant with available protein specific antibodies directed against LKB1 and STRAD $\alpha$  (data not shown). However, if fused to the hexahistidine-tag and using the tag-specific antibody, some faint signal was apparent for LKB1 and STRAD $\alpha$  (Fig. 4B, lanes 2 and 1, respectively), suggesting low abundance of the corresponding proteins in

the soluble bacterial extract. In contrast, MO25 $\alpha$  gave a strong signal if using the tag-specific antibody (Fig. 4B, lane 3). Moreover, a strong band corresponding to MO25 $\alpha$  appeared in all soluble extracts after SDS-PAGE analysis in Coomassie-Blue stained gels (Fig. 4A, lane 1–4), which is consistent with soluble expression of MO25 $\alpha$  in absence of LKB1 and STRAD $\alpha$  (Fig. 2). Importantly, no significant differences between results from different tricistronic constructs were observed, suggesting that the affinity-tag did not affect soluble expression of either subunit.

#### Co-expression of LKB1, MO25 $\alpha$ and STRAD $\alpha$ with chaperones

We have chosen to utilize the tricistronic vector encoding non-tagged MO25 $\alpha$  and STRAD $\alpha$ , and hexahistidine-tagged LKB1 (pHis-LKB1MO25 $\alpha$ STRAD $\alpha$ ) for further studies and analyzed, whether co-expression of bacterial chaperones would result in enhanced solubility of LKB1 by Western-blotting (Fig. 5). Co-expression of DnaK/DnaJ/GrpE increased soluble expression of full-length LKB1

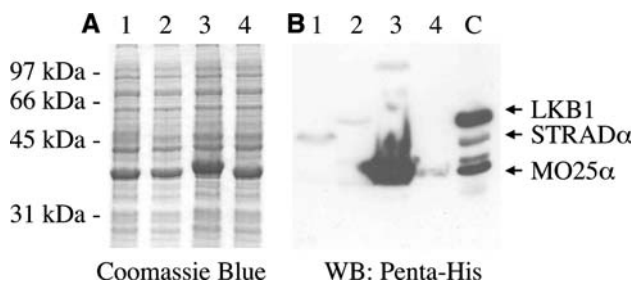


**Fig. 4** Positional effect of hexahistidine-tag on expression of LKB1, MO25 $\alpha$  or STRAD $\alpha$  from tricistronic vectors. The plasmids pLKB1His-STRAD $\alpha$ MO25 $\alpha$  (lanes 1), pHis-LKB1STRAD $\alpha$ MO25 $\alpha$  (lanes 2) or pLKB1STRAD $\alpha$ His-MO25 $\alpha$  (lanes 3), pLKB1STRAD $\alpha$ MO25 $\alpha$  (lanes 4), were transformed to competent *E. coli* and harvested after overnight expression in auto-inducing media. After lysis and centrifugation the soluble bacterial extracts were analyzed by SDS-PAGE. **(A)** Coomassie Blue stained gel. The strong visible band at 40 kDa corresponds to MO25 $\alpha$ , the shift in lane 3 is due to the N-terminally fused hexahistidine-tag. **(B)** Immuno-detection of hexahistidine-tagged proteins after Western-blotting using antibodies raised against the tag. The very strong signal (lane 3) corresponds to MO25 $\alpha$ , whereas LKB1 (lane 2) and STRAD $\alpha$  (lane 1) give only weak signals. The control (lane C) is the same as in Fig. 3, lane 4 (hexahistidine-tagged LKB1, MO25 $\alpha$  and STRAD $\alpha$ , 1  $\mu$ g each)

(Fig. 5B, lane 1 vs. 2), whereas GroES/GroEL reduced the expression level of the full-length protein (Fig. 5B, lane 1 vs. 3). Apparently, co-expression of either chaperone systems also resulted in a number of strong signals at lower molecular weight, likely due to increased proteolysis of LKB1 (Fig. 5B, lanes 2, 3), which are, however, almost absent when the tricistron is expressed without assistance of chaperones (Fig. 5B, lane 1). Therefore, expression of LKB1 complex was pursued without co-expression of bacterial chaperones.

#### Co-expression of LKB1, MO25 $\alpha$ and STRAD $\alpha$ : Purification of the complex

Expression utilizing the tricistronic constructs (Figs. 4 and 5) showed that all three proteins appeared in soluble extracts at least if hexahistidine-tagged, although expression levels of soluble LKB1 and STRAD $\alpha$  were much lower in comparison to MO25 $\alpha$ . Thus, we have chosen to express the tricistronic plasmid encoding hexahistidine-tagged LKB1 at larger scale and to purify proteins chromatographically to explore whether a stable complex between LKB1, MO25 $\alpha$  and STRAD $\alpha$  may have formed. As expected from previous results, no obvious protein bands appeared in the soluble extract at the expected molecular weight of LKB1, as judged from visual inspection of Coomassie Blue-stained gels after SDS-PAGE (Fig. 6A, lane 1). Neither IMAC did result in highly enriched hexahistidine-tagged LKB1 (Fig. 6A, lane 2), although the

tag-specific antibody recognized LKB1 protein at the expected molecular weight in IMAC eluates, giving a somewhat stronger signal than in soluble extracts (Fig. 6E, lanes 1 and 2). For second-step purification, different ion-exchange matrices were tested, however, heparin at slightly basic conditions was found most effective (data not shown). After IMAC and heparin chromatography LKB1, MO25 $\alpha$  and STRAD $\alpha$  were highly enriched as shown by Western-blotting (Fig. 6B–E, lane 3). Still several other protein bands appeared in the eluate (Fig. 6A, lane 3). The unexpected signal at around 70 kDa, which is significantly higher than the molecular weight of STRAD $\alpha$  (Fig. 6D, lanes 1 and 2), disappeared after heparin chromatography (Fig. 6D, lane 3) indicating some unspecificity of the STRAD $\alpha$  antibody. The presence of MO25 $\alpha$  in all fractions (Fig. 6A, lanes 1–3) may only reflect the comparatively higher solubility of MO25 $\alpha$ , which is in excess to LKB1 and STRAD $\alpha$  in soluble extracts and is rather purified away in later steps, reaching roughly equimolar levels with LKB1 and STRAD $\alpha$  after heparin chromatography (Fig. 6, compare signal intensities in lanes 3 and 4 of B, C, D, E, if considering loading of lane 4 is 1  $\mu$ g each). Kinase activity of LKB1 can be determined by incorporation of  $^{32}$ P-phosphate into a synthetic peptide substrate of LKB1, LKBtide [21]. A recent study in our lab utilized an HPLC-based detection method to separate and quantify non-phosphorylated and phosphorylated peptides for activity determination [20]. Here, we modified this method to allow for LKB1 activity measurements using LKBtide. A representative analysis of samples taken at different time points from an LKB1 activity assay is shown in Fig. 7. The enzymatic activities of LKB1 were quantified for each purification step and data are summarized in Table 2. The large proportion of the total LKB1 activity was lost during IMAC and heparin chromatography, as reflected by the low overall yield (5.1%). Nevertheless, in two subsequent purification steps the specific activity increased from 2.3 to 100 U/mg. Most importantly, LKB1 was active in crude bacterial extracts as well as in all elution fractions, suggesting that LKB1 is constitutively active *in vitro*. In our expression and purification scheme only hexahistidine-tagged LKB1 is expected to specifically bind to the IMAC-column and heparin is unlikely to bind LKB1, MO25 $\alpha$  and STRAD $\alpha$  with equal affinity. Thus, co-elution of all three subunits, as shown by Western-blotting after two chromatographic steps, already indicates the formation of a stable protein complex between the three subunits (Fig. 6, lanes 3B–E).

#### Size exclusion chromatography of LKB1 complex

Partly purified, recombinant LKB1 complex corresponding to 120 Units (1.2 mg of the heparin peak elution) was



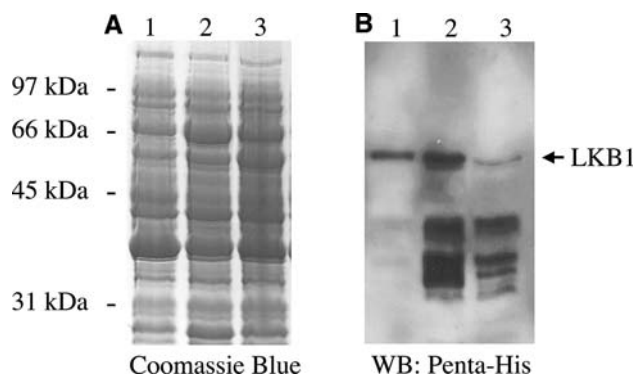


**Fig. 5** Co-expression of bacterial chaperones with a tricistronic vector encoding hexahistidine-tagged LKB1, and non-tagged MO25 $\alpha$  and STRAD $\alpha$ . The tricistronic plasmid (pHis-LKB1MO25 $\alpha$ STRAD $\alpha$ ) was transformed to three different competent *E. coli* cells, without co-expression of chaperones (lane 1), or harbouring pOFXT7-KJE2 for co-expression of DnaJ/DnaK/GrpE (lane 2) or pOFXT7-SL2 for co-expression of GroES/GroEL (lane 3). Cells were harvested after overnight expression in auto-inducing media and lysed by sonication. Soluble bacterial extracts were analyzed by SDS-PAGE. **(A)** Coomassie Blue stained gel. No major differences are seen between samples. **(B)** Immuno-detection of hexahistidine-tagged proteins after Western-blotting. Only LKB1 is fused to the tag and signals corresponding to full-length LKB1 are visible in all lanes to varying degrees. However, additional signals at lower molecular weight appear in samples after co-expression of both bacterial chaperone systems (lanes 2 and 3)

subjected to size exclusion chromatography (SEC) and fractions were collected for further analysis by SDS-PAGE, Western-blotting and activity determination (Fig. 8). The UV-trace of the chromatogram shows three major peaks (Fig. 4A, thick solid line). LKB1 activity eluted between ADH (MW 150 kDa) and  $\beta$ -amylase (MW 200 kDa) marker proteins as a single peak (Fig. 8, broken line), which co-localizes with the first major peak of the UV-trace in the chromatogram. Based on the calibration data (Fig. 8, regression line) this peak corresponds to an apparent molecular weight of 160 kDa. Maximal specific activity in the peak fraction was 250 U/mg (Fig. 8A, fraction 9, marked by an asterisk). Thus, the overall

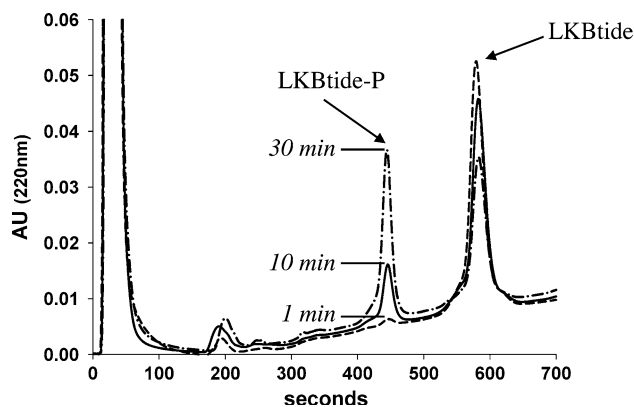


**Fig. 7** LKB1 activity determination. Aliquots of an LKB1 activity assay were taken at different time points as indicated and subjected to ion exchange chromatography using HPLC. The elution profiles show time-dependent increase of phosphorylated LKBtide (LKBtide-P) and concomitant decrease of the non-phosphorylated peptide (LKBtide)

efficiency of the purification strategy is more than 100-fold and is showing a steady increase of specific activities (Fig. 9), and LKB1 activities subjected to SEC were recovered completely (data not shown). LKB1, MO25 $\alpha$  and STRAD $\alpha$  exactly co-eluted from the column as shown by Western-blotting using specific antibodies (Fig. 8B). Moreover, the fractions exhibiting the highest specific activities also show highest signal intensities for LKB1, MO25 $\alpha$  and STRAD $\alpha$  (Fig. 8B), again indicating the formation of a stable LKB1-MO25 $\alpha$ -STRAD $\alpha$  complex. Inspection of the Coomassie Blue-stained gel after separation of the SEC column fractions also reveals visible staining at the expected molecular weight of LKB1, MO25 $\alpha$  and STRAD $\alpha$ . These protein bands coincide and co-localize with the Western-blot signals, suggesting that all three proteins have reached detectable levels with this staining method. Based on correct identification of the protein bands, densitometric analysis indicates that the overall purity of LKB1-MO25 $\alpha$ -STRAD $\alpha$  complex in fraction 9 is approx. 25%.

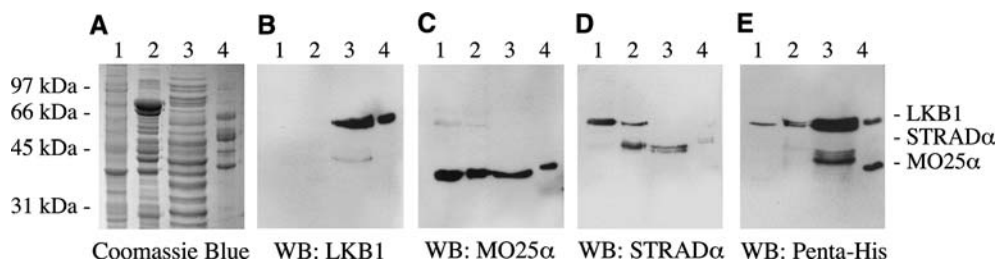


**Fig. 6** Purification of LKB1 complex. Cells were lysed and centrifuged after bacterial co-expression of untagged MO25 $\alpha$ , STRAD $\alpha$  and hexahistidine-tagged LKB1, using the tricistronic expression vector pHis-LKB1MO25 $\alpha$ STRAD $\alpha$ . The supernatant representing the soluble extract was subjected to sequential IMAC and heparin chromatography. Soluble extract, IMAC eluate, Heparin

eluate and control proteins were analyzed by SDS-PAGE followed by Coomassie-Blue staining **(A)** or Western-blotting **(B-E)**. Separate Western-blot were prepared for probing with four different antibodies as indicated. Lane 1, soluble extract (20  $\mu$ g); lane 2, IMAC eluate (20  $\mu$ g); lane 3, heparin eluate (20  $\mu$ g); lane 4: LKB1, MO25 $\alpha$  and STRAD $\alpha$  (1  $\mu$ g each, the same sample as in Fig. 3, lane 4)

**Table 2** Summary of purification of recombinant LKB1-MO25 $\alpha$ -STRAD $\alpha$ 

Fraction	Total activity (U) <sup>a</sup>	Total protein (mg)	Specific activity (U/mg)	Purification (fold)	Yield (%)
Lysate	19320	8400	2.3	1	100
IMAC	3386	102	33.2	14.4	17.5
Heparin	986	9.8	100.7	43.8	5.1

<sup>a</sup> One Unit is defined as 1 nmole phosphate incorporated into LKBtide per minute

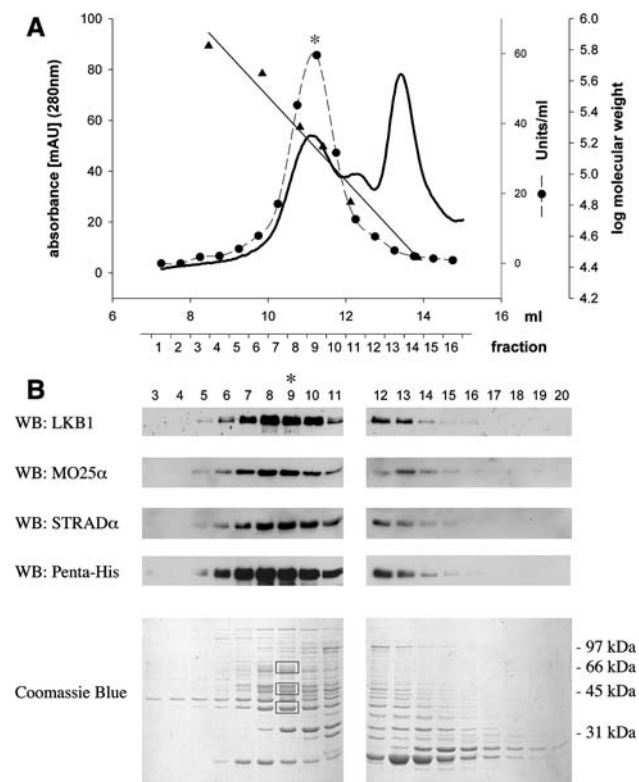


**Fig. 8** Size exclusion chromatography of partly purified LKB1 complex. 120 U (1.2 mg of the heparin elution peak fraction) were separated on a Superose-12 HR 10/30 column. **(A)** The UV-trace (thick solid line) gives the absorption at 280 nm (left scale). Elution fractions (0.5 ml each) were collected and analyzed for LKB1 activity (filled circles with broken line, inner right axis). The column was calibrated for molecular weight by different marker proteins (triangles with regression line, outer right axis). The highest specific activity of 250 U/mg elutes in fraction 9 (marked by an asterisk) at an apparent molecular weight of 160 kDa. **(B)** Elution fractions of the size exclusion column were further analyzed by SDS-PAGE and Western-blotting using antibodies as indicated. Hexahistidine-tagged LKB1, MO25 $\alpha$  and STRAD $\alpha$  proteins co-elute and the strongest signal intensities are observed in elution fractions exhibiting the highest LKB1 activities as shown in **(A)**. Coomassie Blue-stained protein bands that likely represent LKB1, STRAD $\alpha$  and MO25 $\alpha$  are framed (top to bottom)

### LKB1 complex phosphorylates and activates AMPK

A physiological target of LKB1 was recently identified as AMP-activated protein kinase (AMPK) [11–13]. We used recombinant AMPK that is almost entirely inactive to

verify the ability of LKB1 complex to activate AMPK by phosphorylation at Thr-172 of the catalytic  $\alpha$ -subunit. Incorporation of radioactivity into the  $\alpha$ - and  $\beta$ - subunits of AMPK in presence, but not in absence of LKB1 complex indicates phosphorylation of AMPK by LKB1 (Fig. 10B, lanes 3, 5). Kinase-defective mutant AMPK  $\alpha$ 1-complex incorporates radioactivity only into the catalytic AMPK  $\alpha$ -subunit, showing that LKB1 is phosphorylating exclusively the  $\alpha$ -subunit (Fig. 10B, lane 7). The absence of  $\beta$ -subunit phosphorylation in kinase dead AMPK after incubation with LKB1 is reflecting the inability of the AMPK mutant to autophosphorylate after activation. Finally, Western-blotting using antibodies recognizing phosphorylated AMPK  $\alpha$  Thr-172 (Fig. 10C) and activity determination (Fig. 10D) confirms phosphorylation at Thr-172 that is a pre-requisite of significant AMPK activity [20].

### Discussion

LKB1 is known to interact with MO25 and STRAD *in vivo* [4, 21]. Here, we show that the components of the LKB1 complex can be individually expressed, but with the exception of MO25 $\alpha$ , both LKB1 and STRAD $\alpha$  are found insoluble in inclusion bodies. Since subunits of protein complexes often require their natural binding partners for correct folding and solubility [22], we attempted co-expression of all three proteins in bacteria, which turned out to be a useful strategy for isolation of the functional LKB1 complex from soluble extracts. The three polypeptides were identified as LKB1, MO25 $\alpha$  and STRAD $\alpha$  by their apparent molecular weight, as determined by SDS-PAGE and their reactivity with specific antibodies. MO25 $\alpha$  and STRAD $\alpha$  co-eluted with hexahistidine-tagged LKB1 from the immobilized metal-ion affinity (IMAC) and heparin columns. In size exclusion chromatography (SEC), the highest LKB1 activities eluted at an apparent molecular weight of 160 kDa (Fig. 8A), which is consistent with complex-formation. Moreover, MO25 $\alpha$  and STRAD $\alpha$  exactly co-eluted with LKB1 from the size exclusion column as shown by Western-blotting (Fig. 8B). Thus, we presume that the LKB1, MO25 $\alpha$ (and STRAD $\alpha$  proteins assemble into a 1:1:1 heterotrimeric complex in the cytoplasm of *E. coli*. Additionally, we show that recombinant

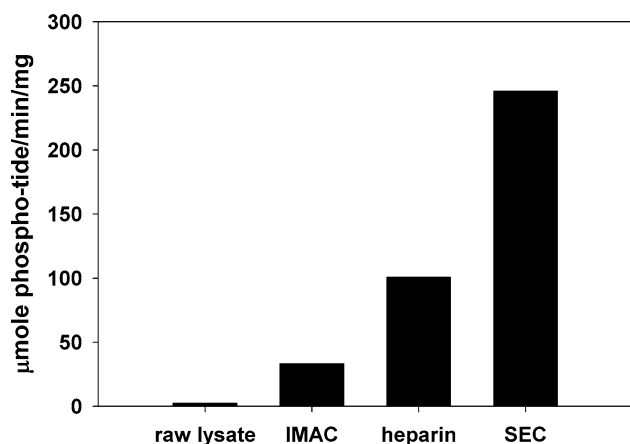


**Fig. 9** Specific activities of LKB1 in different elution fractions. Each bar represents activity values that were calculated from a chromatogram (area under the curve) of a single HPLC run as shown in Fig. 7

LKB1 complex is capable of phosphorylating AMPK at Thr-172 of the  $\alpha$ -subunit, as was reported for the native enzyme previously [13], and this phosphorylation also leads to strongly increased activity of AMPK. We therefore

conclude that recombinant LKB1-MO25 $\alpha$ -STRAD $\alpha$  is fully functional. In contrast to AMPK purified from bacteria, which is inactive unless activated by either of its upstream kinases [9], the recombinant LKB1 complex is highly active and strongly autophosphorylates after extraction. Importantly, neither activation by upstream kinases, nor other posttranslational modifications, like C-terminal farnesylation of LKB1 [23], that may either not be performed at all or only incorrectly by *E. coli*, were critical for enzyme activity or stability of the complex, supporting the notion that LKB1 is constitutively active *in vitro*. Such constitutive activity of the LKB1 complex *in vivo* has been recently suggested [3], but not experimentally proven.

Using tricistronic vectors, we explored the positional effect of the N-terminal hexahistidine-tag on soluble expression of the LKB1 complex. Soluble expression of LKB1 and STRAD $\alpha$  proteins could only be assessed if the corresponding protein was hexahistidine-tagged and using antibodies recognizing the tag, which revealed low but comparable signal intensities for full-length tagged LKB1 and tagged STRAD $\alpha$ . Hence, if present at all, positional

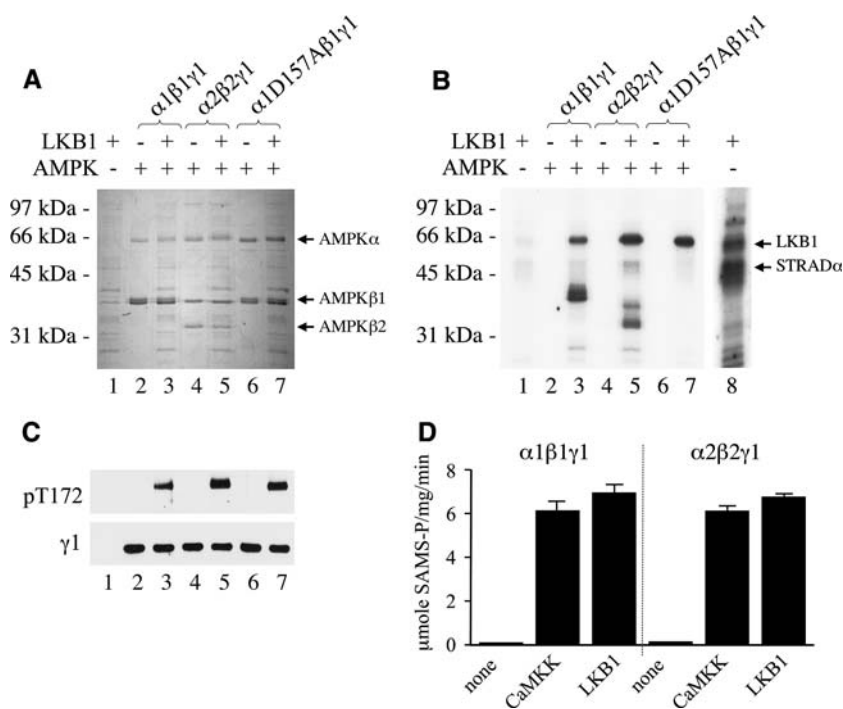


**Fig. 10** Autophosphorylation LKB1-MO25 $\alpha$ -STRAD $\alpha$  and activation of AMPK. **(A)** Coomassie Blue-stained gel. **(B)** LKB1 and STRAD $\alpha$  strongly autophosphorylate, as shown by autoradiography after incubation with radioactive ATP (lane 8), but pre-incubation of LKB1 complex with non-radioactive ATP (lane 1–7) suppresses signals derived from such autophosphorylation. No radioactivity is incorporated in AMPK in absence of LKB1 (lanes 2, 4, 6), but clear signals appear if LKB1 is allowed to phosphorylate AMPK (lanes 3, 5, 7). In wild-type AMPK the  $\beta$ -subunits are labelled in addition to  $\alpha$ -subunits (lanes 3, 5), but in kinase-defective mutant AMPK (D157A,

Asp-157 replaced with Ala), which is unable to autophosphorylate, only the  $\alpha$ -subunit is incorporating radioactivity (lane 7). **(C)** Western blot of the same samples as in **(A)** using a phospho-specific Thr-172 antibody, showing that AMPK is phosphorylated by LKB1 complex at this activating site (lanes 3, 5, 7). The  $\gamma$ -subunit signals are comparable in lanes 2–7 showing equal loading of AMPK. **(D)** Activity determination of two different AMPK isoforms ( $\alpha$ 1 $\beta$ 1 $\gamma$ 1 and  $\alpha$ 2 $\beta$ 2 $\gamma$ 1) before and after addition of upstream kinases (CaMKK $\beta$  or LKB1). Results are mean S.D. ( $n = 3$ )

effects are rather small and not detectable using the methods applied here. We also addressed whether co-expression of chaperones would augment soluble expression of LKB1-MO25 $\alpha$ -STRAD $\alpha$  and essentially found increased signal intensities corresponding to lower molecular weight products of LKB1, strongly suggesting enhanced degradation rather than chaperone-assisted folding and assembly of the complex, which is consistent with the cellular roles of molecular chaperones and proteases for *de novo* folding and quality control of proteins [24].

Densitometric analysis revealed an approximate purity of 25% for the LKB1-MO25 $\alpha$ -STRAD $\alpha$  complex in the LKB1 peak elution fraction after SEC (Fig. 8B, fraction 9, boxed areas). The same SEC fraction also exhibited the maximal specific activity of 250 U/mg, suggesting that homogeneous LKB1 complex would exhibit around 1000 U/mg. The specific activities of bacterially expressed LKB1 complex are, however, difficult to compare with previous preparations from rat liver [25] that appeared to contain LKB1 [11], but were reported prior to the development of LKBtide [5]. Co-expression of GST-fusions of LKB1, MO25 $\alpha$  and STRAD $\alpha$  in HEK293 cells and affinity purification results in significantly lower specific activities around 20 U/mg [21], but the purity of these preparations remains elusive.

In this study, we also developed a new method for quantitation of LKB1 activity from kinase assays using the synthetic peptide substrate, LKBtide [5]. We determined the amount of phosphorylated LKBtide by HPLC analysis using non-radioactive ATP, thereby avoiding the use of radioactivity and scintillation counting. In our opinion, the HPLC method is very reliable and accurate, which justifies its use in this and future studies, even though the traditional radioactive method is less time consuming and many activity determinations can be performed in parallel.

Co-expression of proteins in bacteria has recently gained significant interest since rather assemblies of proteins than single macromolecules form the functional units of the eukaryotic cell, and one major challenge of the post-genomic era is to produce these complexes in sufficient amounts to be studied by biochemical and structural means [22]. It should be emphasized that the virtual absence of the common eukaryotic posttranslational modifications in bacteria, especially phosphorylation by endogenous kinases, constitutes a major advantage of bacterial over-expression. Undoubtedly, such wanted or unwanted posttranslational modifications frequently occur after over-expression in yeast, insect or mammalian cell based expression systems, with the clear disadvantage that assignment of a biological function to a certain modification can be obscured. Thus, the LKB1 complex from bacteria offers a unique perspective of studying the effect of posttranslational modifications on the molecular level and provides a versatile reagent for biochemical experimentation.

**Acknowledgements** We thank Dario Alessi for the provision of cDNAs, Oliver Fayet for plasmids and Uwe Schlattner for discussion. The work was supported by Novartis Foundation No. 05A07 and Helmut Horten Foundation (to D.N., T.W.) and by an ETH graduate student grant for R.T. given to T. W. Further, the study was supported by Swiss National Science Foundation No 3100AO-102075 and FP6 contract LSHM-CT-2004-005272 (EXGENESIS) (to T.W. and Uwe Schlattner).

## References

- Hemminki, A., Markie, D., Tomlinson, I., Avizienyte, E., Roth, S., Loukola, A., Bignell, G., Warren, W., Aminoff, M., Hoglund, P., Jarvinen, H., Kristo, P., Pelin, K., Ridanpaa, M., Salovaara, R., Toro, T., Bodmer, W., Olschwang, S., Olsen, A. S., Stratton, M. R., de la Chapelle, A., & Aaltonen, L. A. (1998). A serine/threonine kinase gene defective in Peutz-Jeghers syndrome. *Nature*, *391*(6663), 184–187.
- Jenne, D. E., Reimann, H., Nezu, J., Friedel, W., Loff, S., Jeschke, R., Muller, O., Back, W., & Zimmer, M. (1998). Peutz-Jeghers syndrome is caused by mutations in a novel serine threonine kinase. *Nature Genetics*, *18*(1), 38–43.
- Alessi D. R., Sakamoto K., & Bayascas, J. R. (2006). LKB1-dependent signaling pathways. *Annual Review of Biochemistry*, *75*, 137–163.
- Boudeau, J., Baas, A. F., Deak, M., Morrice, N. A., Kieloch, A., Schutkowski, M., Prescott, A. R., Clevers, H. C., & Alessi, D. R. (2003). MO25 $\alpha$ /beta interact with STRAD $\alpha$ /beta enhancing their ability to bind, activate and localize LKB1 in the cytoplasm. *The Embo Journal*, *22*(19), 5102–5114.
- Lizcano, J. M., Goransson, O., Toth, R., Deak, M., Morrice, N. A., Boudeau, J., Hawley, S. A., Udd, L., Makela, T. P., Hardie, D. G., & Alessi, D. R. (2004). LKB1 is a master kinase that activates 13 kinases of the AMPK subfamily, including MARK/PAR-1. *The Embo Journal*, *23*(4), 833–843.
- Jaleel, M., McBride, A., Lizcano, J. M., Deak, M., Toth, R., Morrice, N. A., & Alessi, D. R. (2005). Identification of the sucrose non-fermenting related kinase SNRK, as a novel LKB1 substrate. *FEBS Letters*, *579*(6), 1417–1423.
- Martinez-Torrecuadrada, J. L., Romero, S., Nunez, A., Alfonso, P., Sanchez-Cespedes, M., & Casal, J. I. (2005). An efficient expression system for the production of functionally active human LKB1. *Journal of Biotechnology*, *115*(1), 23–34.
- Neumann, D., Schlattner, U., & Wallimann, T. (2003). A molecular approach to the concerted action of kinases involved in energy homeostasis. *Biochemical Society Transactions*, *31*(Pt 1), 169–174.
- Neumann, D., Woods, A., Carling, D., Wallimann, T., & Schlattner, U. (2003). Mammalian AMP-activated protein kinase: functional, heterotrimeric complexes by co-expression of subunits in *Escherichia coli*. *Protein Expression and Purification*, *30*(2), 230–237.
- Carling, D. (2005). AMP-activated protein kinase: balancing the scales. *Biochimie*, *87*(1), 87–91.
- Hawley, S. A., Boudeau, J., Reid, J. L., Mustard, K. J., Udd, L., Makela, T. P., Alessi, D. R., & Hardie, D. G. (2003). Complexes between the LKB1 tumor suppressor, STRAD  $\alpha$ /beta and MO25  $\alpha$ /beta are upstream kinases in the AMP-activated protein kinase cascade. *Journal of Biology*, *2*(4), 28.
- Shaw, R. J., Kosmatka, M., Bardeesy, N., Hurley, R. L., Witters, L. A., DePinho, R. A., Cantley, L. C. (2004). The tumor suppressor LKB1 kinase directly activates AMP-activated kinase and regulates apoptosis in response to energy stress. *Proceedings of the National Academy of Sciences of the United States of America*, *101*(10), 3329–3335.



13. Woods, A., Johnstone, S. R., Dickerson, K., Leiper, F. C., Fryer, L. G., Neumann, D., Schlattner, U., Wallimann, T., Carlson, M., & Carling, D. (2003). LKB1 is the upstream kinase in the AMP-activated protein kinase cascade. *Current Biology*, *13*(22), 2004–2008.
14. Sakamoto, K., McCarthy, A., Smith, D., Green, K. A., Grahame Hardie, D., Ashworth, A., & Alessi, D. R. (2005). Deficiency of LKB1 in skeletal muscle prevents AMPK activation and glucose uptake during contraction. *The Embo Journal*, *24*(10), 1810–1820.
15. Corradetti, M. N., Inoki, K., Bardeesy, N., DePinho, R. A., & Guan, K. L. (2004). Regulation of the TSC pathway by LKB1: evidence of a molecular link between tuberous sclerosis complex and Peutz-Jeghers syndrome. *Genes & Development*, *18*(13), 1533–1538.
16. Inoki, K., Zhu, T., & Guan, K. L. (2003). TSC2 mediates cellular energy response to control cell growth and survival. *Cell*, *115*(5), 577–590.
17. Shaw, R. J., Bardeesy, N., Manning, B. D., Lopez, L., Kosmatka, M., DePinho, R. A., & Cantley, L. C. (2004). The LKB1 tumor suppressor negatively regulates mTOR signaling. *Cancer Cell*, *6*(1), 91–99.
18. Studier, F. W. (2005). Protein production by auto-induction in high density shaking cultures. *Protein Expr Purif*, *41*(1), 207–234.
19. Castanie, M. P., Berges, H., Oreglia, J., Prere, M. F., & Fayet, O. (1997). A set of pBR322-compatible plasmids allowing the testing of chaperone-assisted folding of proteins overexpressed in *Escherichia coli*. *Analytical of Biochemistry*, *254*(1), 150–152.
20. Suter M., Riek U., Tuerk R., Schlattner U., Wallimann T., & Neumann, D. (2006). Dissecting the role of 5'-AMP for allosteric stimulation, activation, and deactivation of AMP-activated protein kinase. *Journal of Biological Chemistry*, *281*(43), 32207–32216.
21. Boudeau, J., Scott, J. W., Resta, N., Deak, M., Kieloch, A., Komander, D., Hardie, D. G., Prescott, A. R., van Aalten, D. M., & Alessi, D. R. (2004). Analysis of the LKB1-STRAD-MO25 complex. *Journal of Cell Science*, *117*(Pt 26), 6365–6375.
22. Romier, C., Ben Jelloul, M., Albeck, S., Buchwald, G., Busso, D., Celie, P. H., Christodoulou, E., De Marco, V., van Gerwen, S., Knipscheer, P., Lebbink, J. H., Notenboom, V., Poterszman, A., Rochel, N., Cohen, S. X., Unger, T., Sussman, J. L., Moras, D., Sixma, T. K., & Perrakis, A. (2006). Co-expression of protein complexes in prokaryotic and eukaryotic hosts: experimental procedures, database tracking and case studies. *Acta Crystallographica Section D, Biological Crystallography*, *62*(Pt 10), 1232–1242.
23. Sapkota, G. P., Kieloch, A., Lizcano, J. M., Lain, S., Arthur, J. S., Williams, M. R., Morrice, N., Deak, M., & Alessi, D. R. (2001). Phosphorylation of the protein kinase mutated in Peutz-Jeghers cancer syndrome, LKB1/STK11, at Ser431 by p90(RSK) and cAMP-dependent protein kinase, but not its farnesylation at Cys(433), is essential for LKB1 to suppress cell growth. *Journal of Biological Chemistry*, *276*(22), 19469–19482.
24. Tomoyasu, T., Mogk, A., Langen, H., Goloubinoff, P., & Bukau, B. (2001). Genetic dissection of the roles of chaperones and proteases in protein folding and degradation in the *Escherichia coli* cytosol. *Molecular Microbiology*, *40*(2), 397–413.
25. Hawley, S. A., Davison, M., Woods, A., Davies, S. P., Beri, R. K., Carling, D., & Hardie, D. G. (1996). Characterization of the AMP-activated protein kinase from rat liver and identification of threonine 172 as the major site at which it phosphorylates AMP-activated protein kinase. *Journal of Biological Chemistry*, *271*(44), 27879–27887.